

Space structure of the EGAM modes in TCV, experimental observations and modeling

M. Dreval, A. Biancalani, T. Hayward-Schneider, A. Mishchenko, A.N. Karpushov, A. Jansen van Vuuren, U.A. Sheikh, D. Gossard, S.E. Sharapov, B. Rofman, L.Villard and the TCV Team*

WPTE RT09 and TSVV-G: Physics of Burning Plasmas

TCV

* See *See Duval et al 2024*



This work has been carried out within the framework of the EUROfusion Consortium and has received funding from the Euratom research and training programme 2014-2018 under grant agreement No 633053. The views and opinions expressed herein do not necessarily reflect those of the European Commission.

TSVV-G seminar, Feb. 23 2026

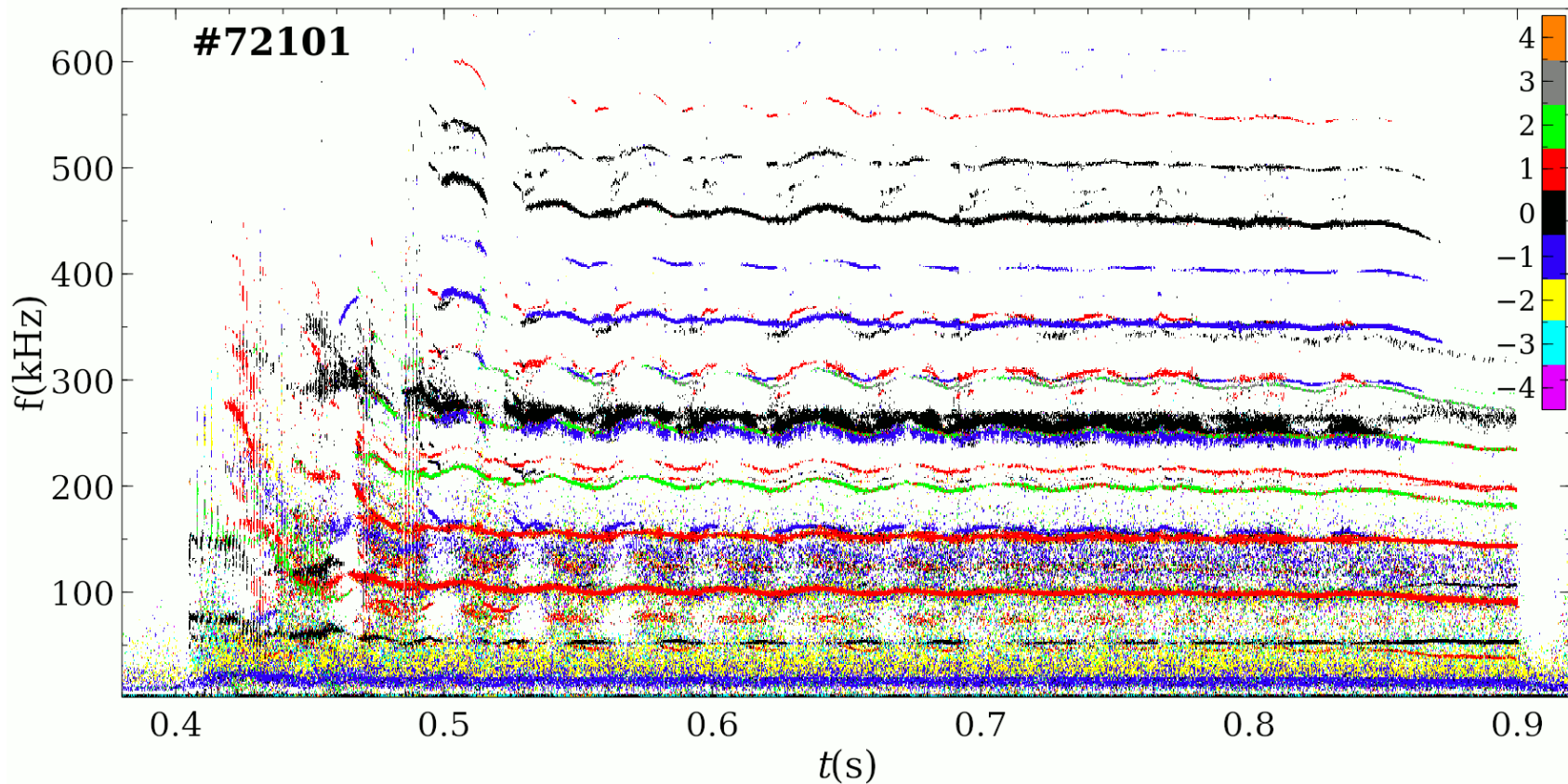


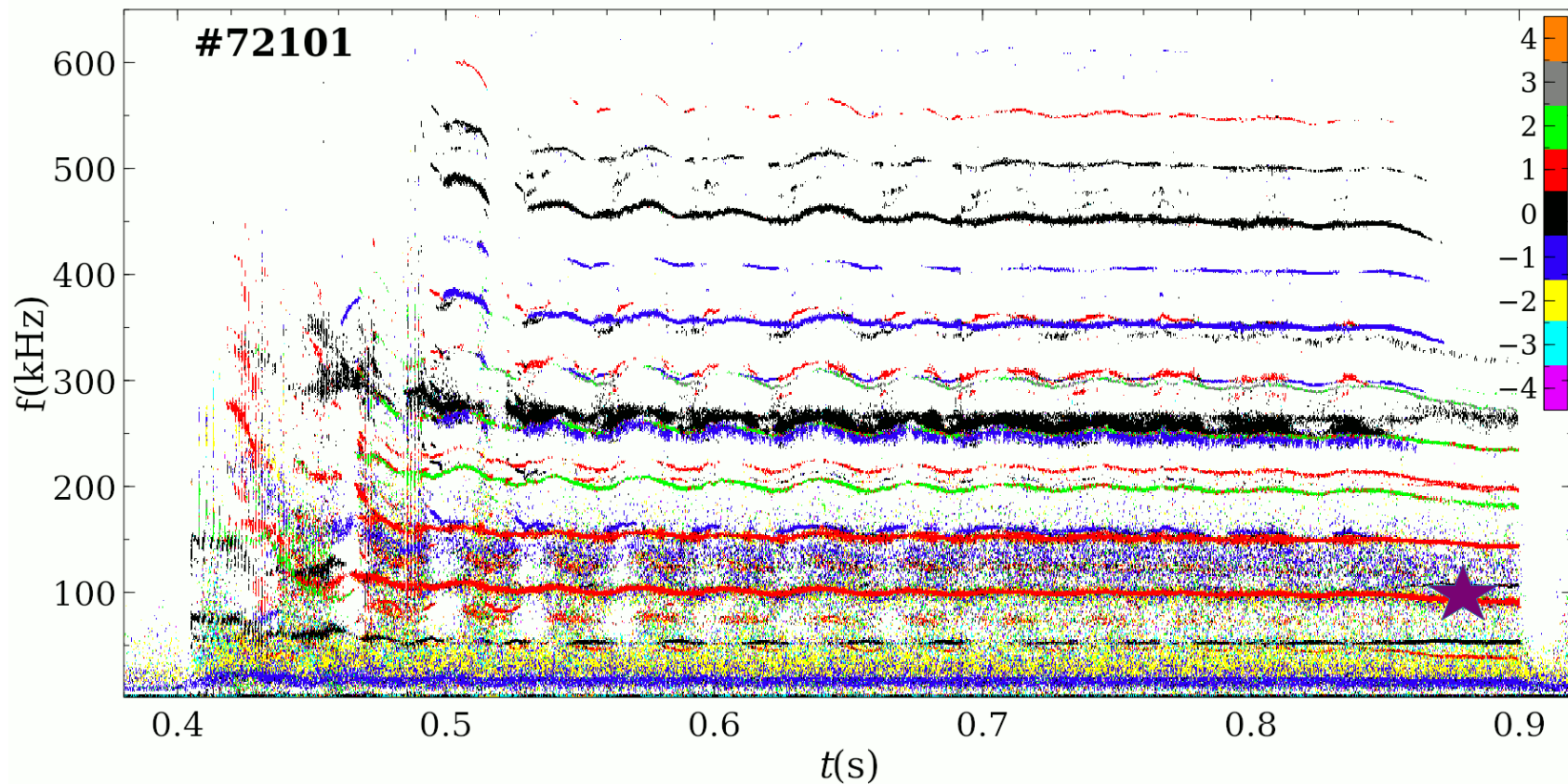
- Synergy :
to RT09 – advanced modeling from TSVV
to TSVV – codes validation
- Contents

Information of my activity in RT09 framework

Techniques of modes description by SXR , Magnetics

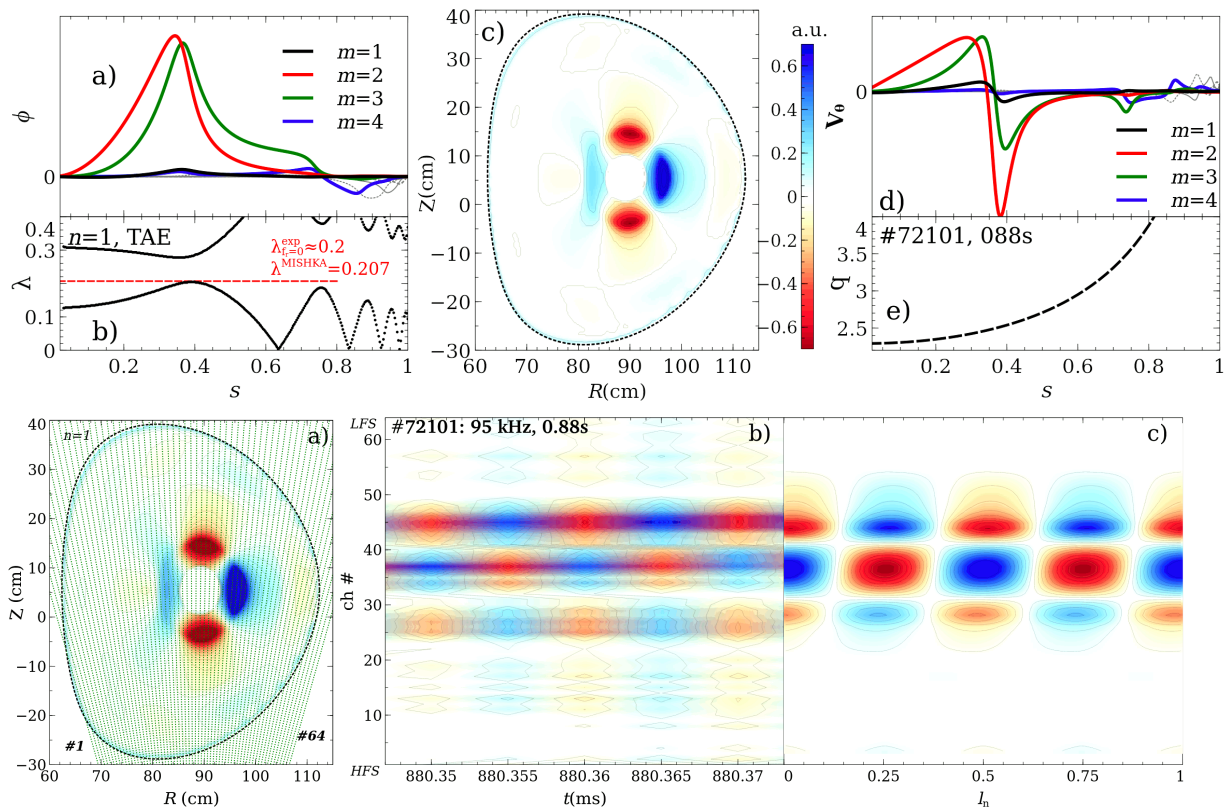
“SXR” diagnostics for ORB5, “Magnetic” diagnostics for ORB5

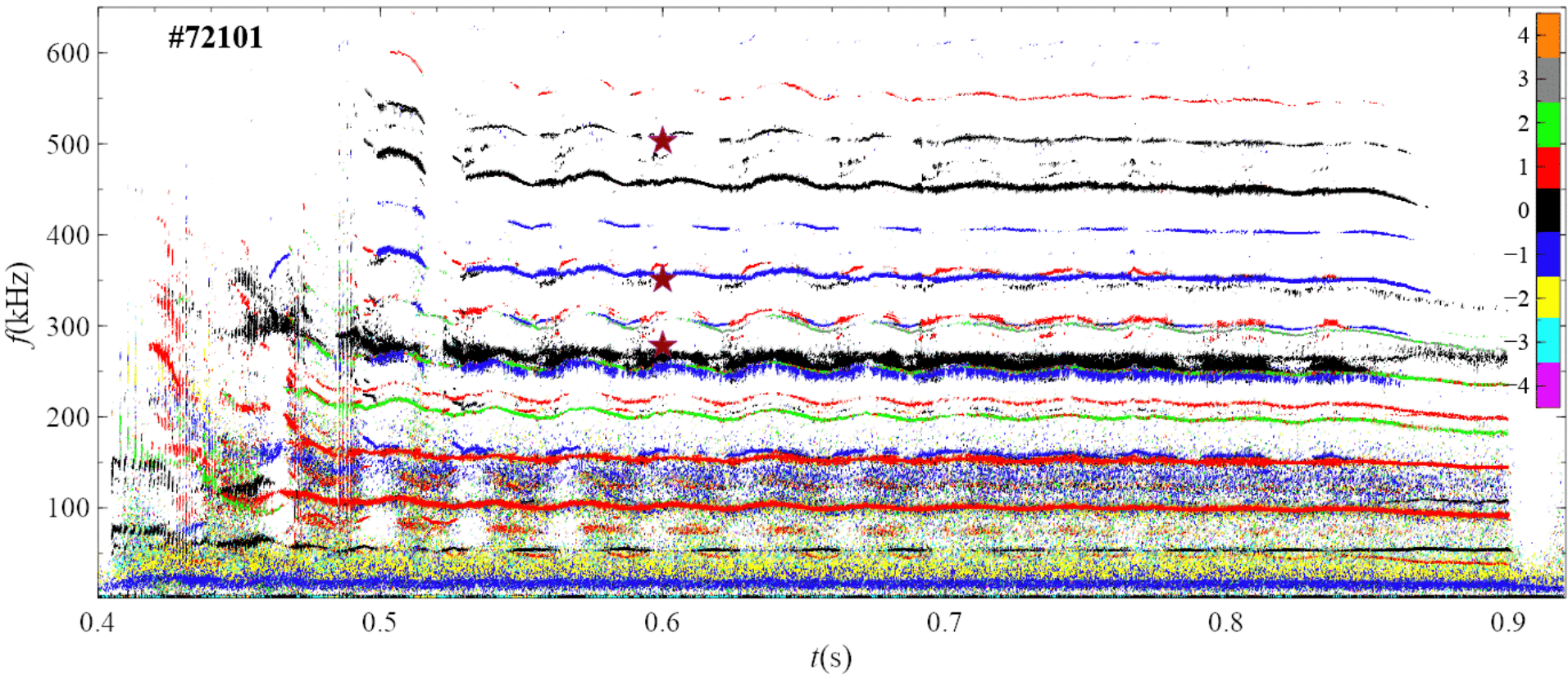


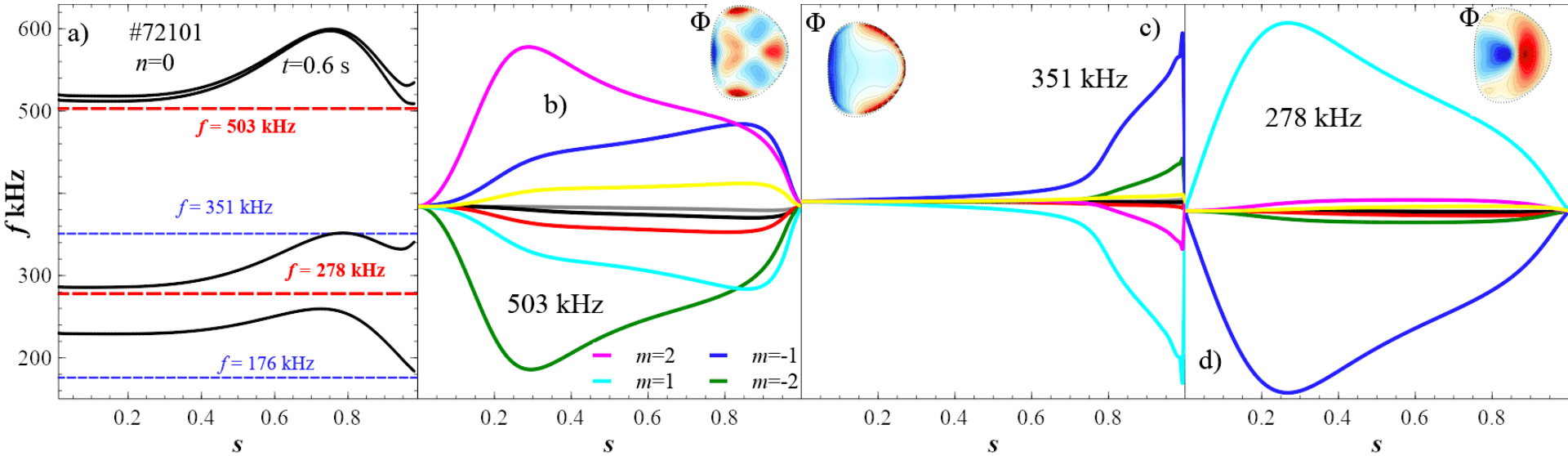


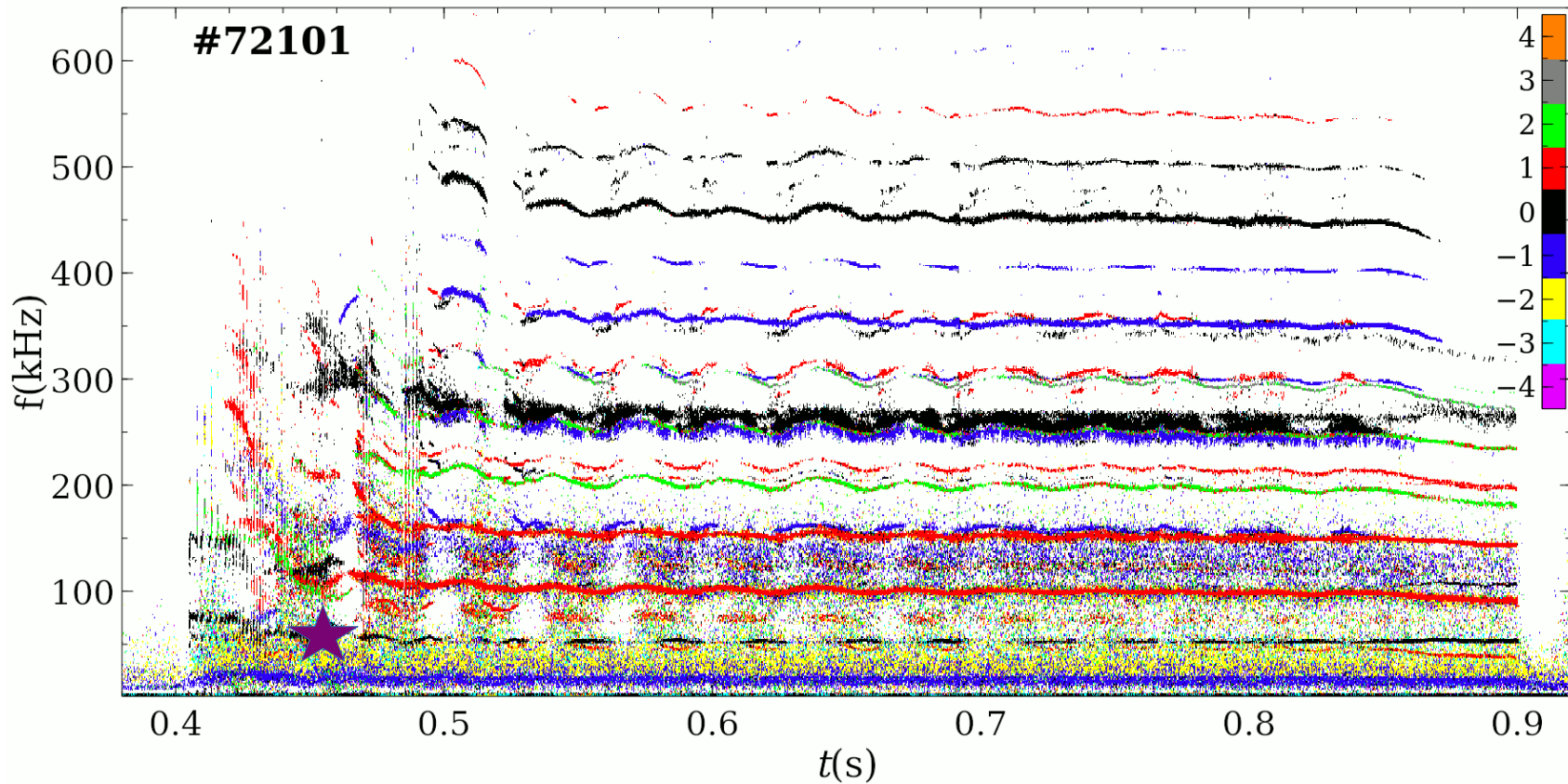


Info:TAE by MISHKA + SXR forward modeling¹



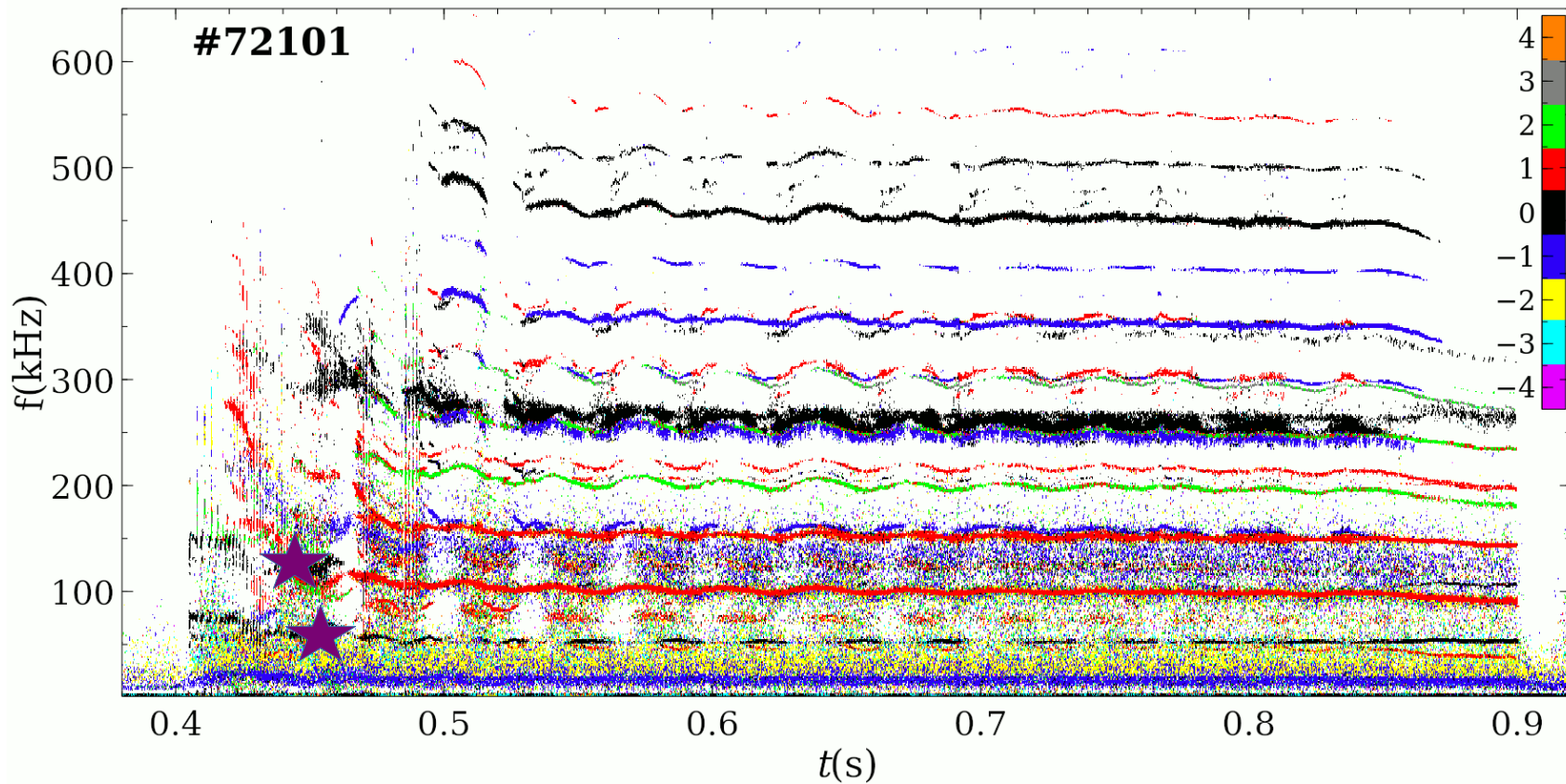


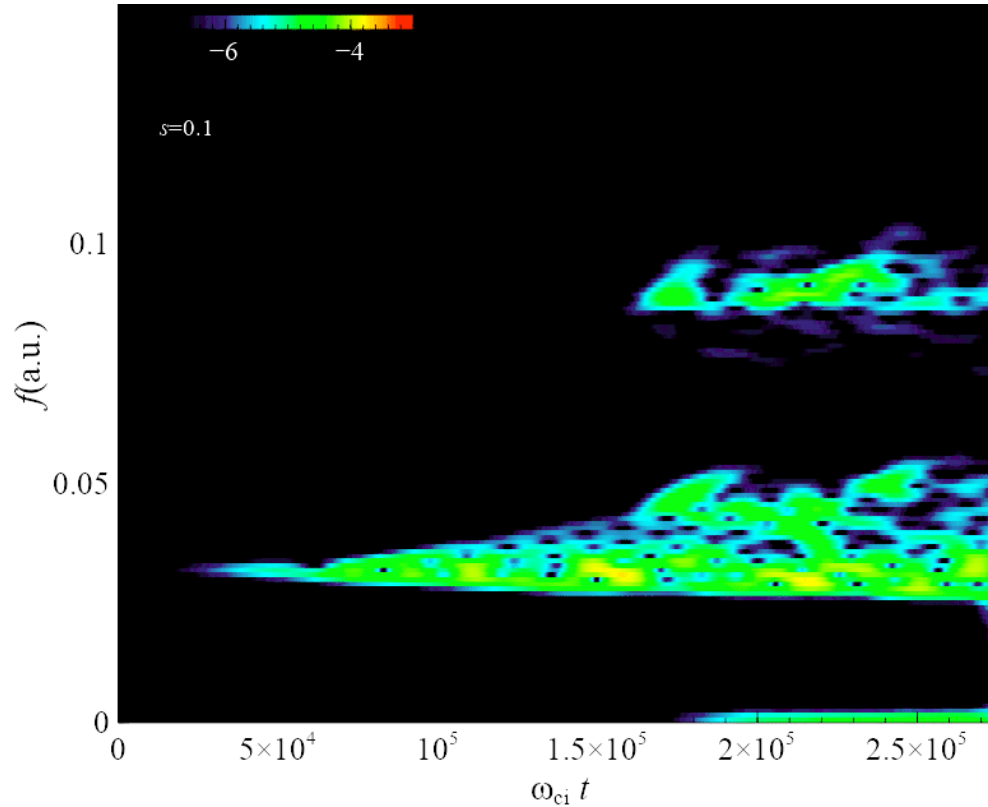




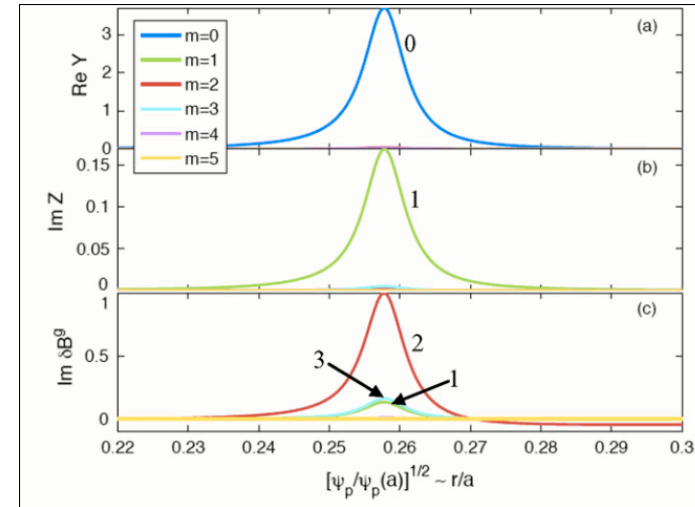
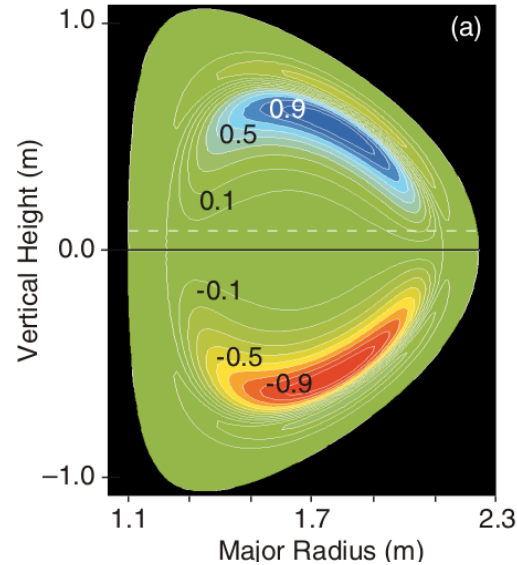
³M.B. Dreval et al., 2025 Nucl. Fusion **65** 016037

⁴M.B. Dreval et al., EUROfusion pinboard 2025 #589





EGAM: Introduction: EGAM vs fast particles driven GAM vs GAM



EGAM¹ as well as GAM

- $n=0$

- $m=1$ standing wave localized vertically for n_e

¹Nazikian R. et al 2008 Phys. Rev. Lett. **101** 185001

²Berk H.L. et al 2006 Nucl. Fusion **46** S888

³L. Horváth et al 2016 Nucl. Fusion **56** 112003

- **$m=2$** of Magnetic field oscillations at plasma edge (c)²

- fast particles pressure gradient impact overcome main plasma pressure impact => EGAM (EMPs)^{2,3}

-EGAM frequency can be different to GAM (0.5 of GAM frequency in¹)

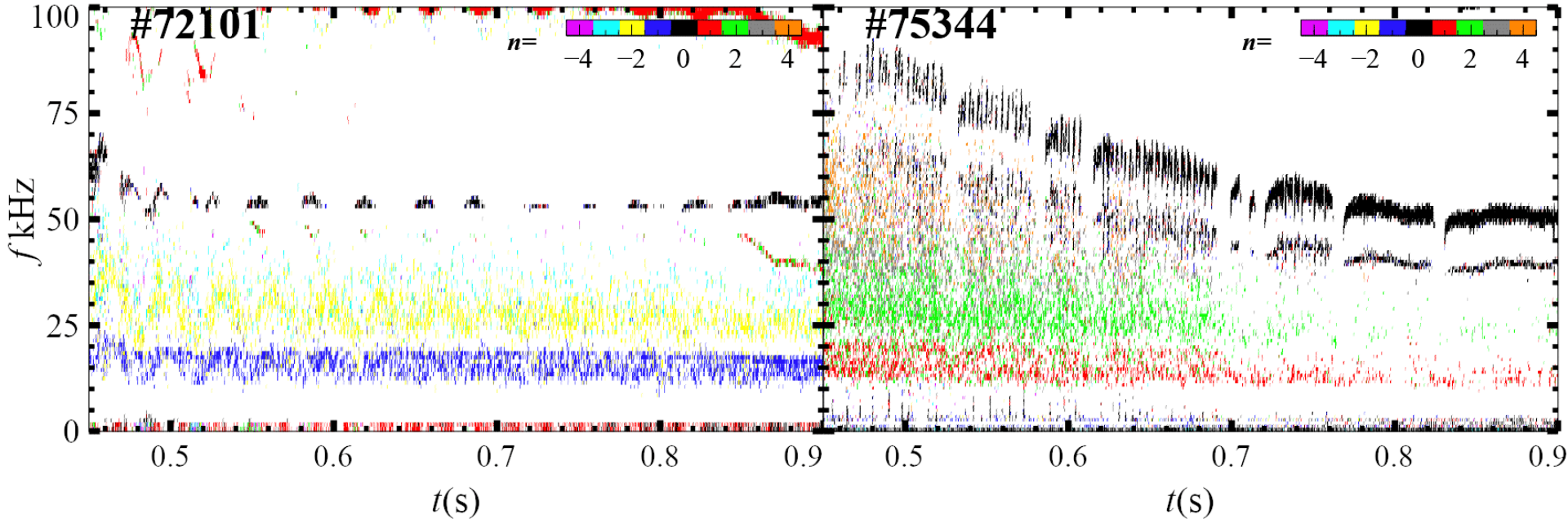


Fig.1 Toroidal mode numbers n in TCV pulses #72101 ($B_0 = +1.3$ T, $I_p = +120$ kA) and #75344 ($B_0 = -1.45$ T, $I_p = -150$ kA). Two different frequencies of the EGAMs is observed in #75344 shot.

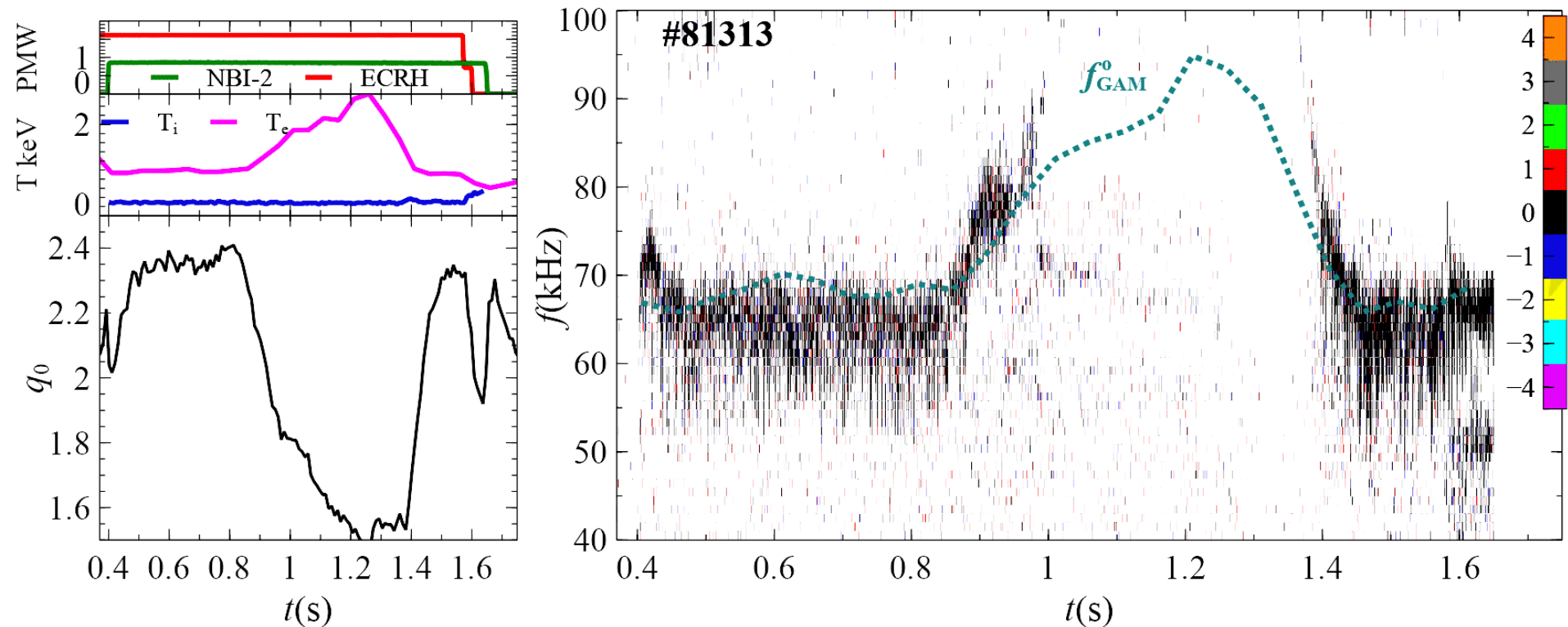


Fig.2 #81313 ($B_0 = -1.45$ T, $I_p = -120$ kA), NBI-2 and ECRH power, central ion and electron temperatures, central safety factor from magnetic LIUQE equilibrium. Toroidal mode numbers (n) are evaluated by radial-component magnetic LTCC coils with central GAM frequency calculated by Eq.1 from Ref. [1].

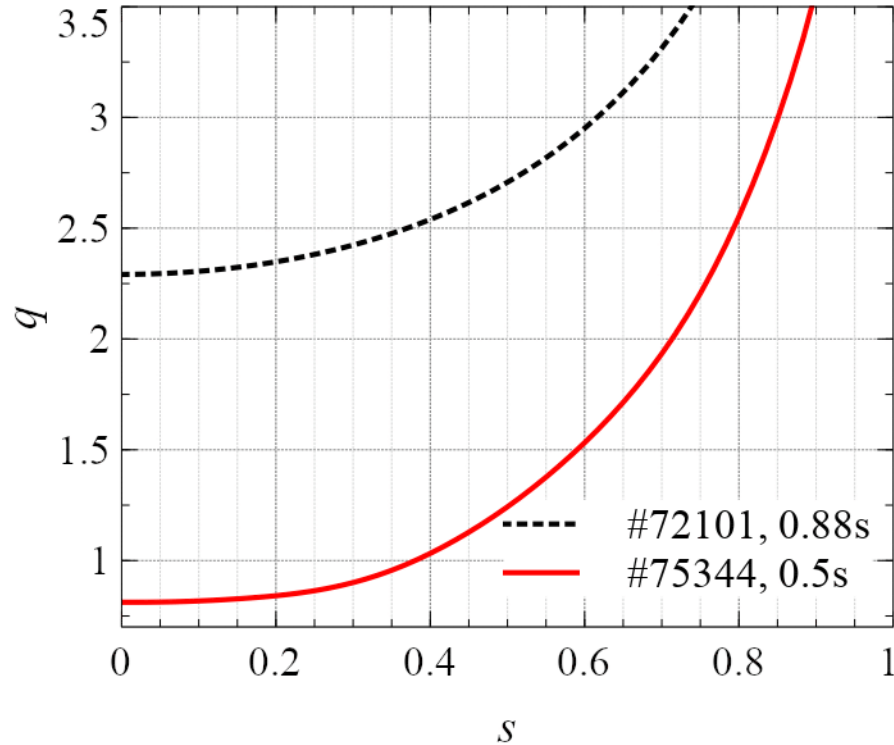


Fig.5 Radial profiles of safety factor in TCV discharge #75344 at 0.5s. (in red) and TCV discharge #72101 at 0.88s. (in black, dashed line) .

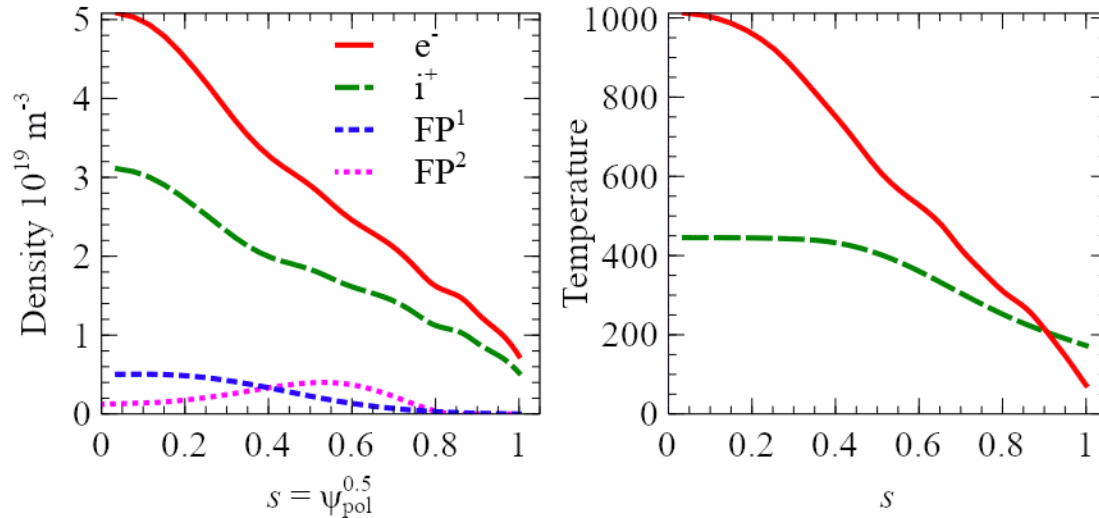


Fig.4 Radial profiles of ion and electron temperature and density. In addition, two modeling profiles of fast particles density are shown corresponding to different NBI scenarios (on-axis vs. off-axis).

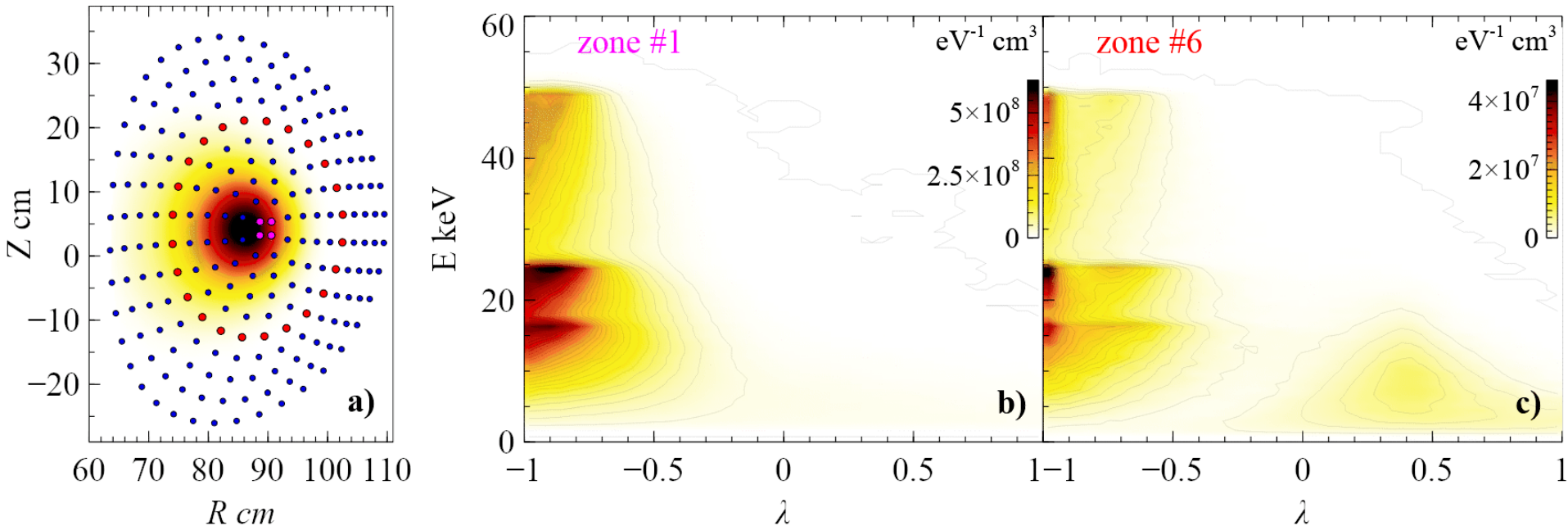


Fig.3 a) TRANSP cells (in blue) and distribution of 45-49 keV averaged fast ions in poloidal cross-section, zone-averaged FP distributions for zones #1 (b) and #6 (c). TCV discharge #75344 at 0.5s.

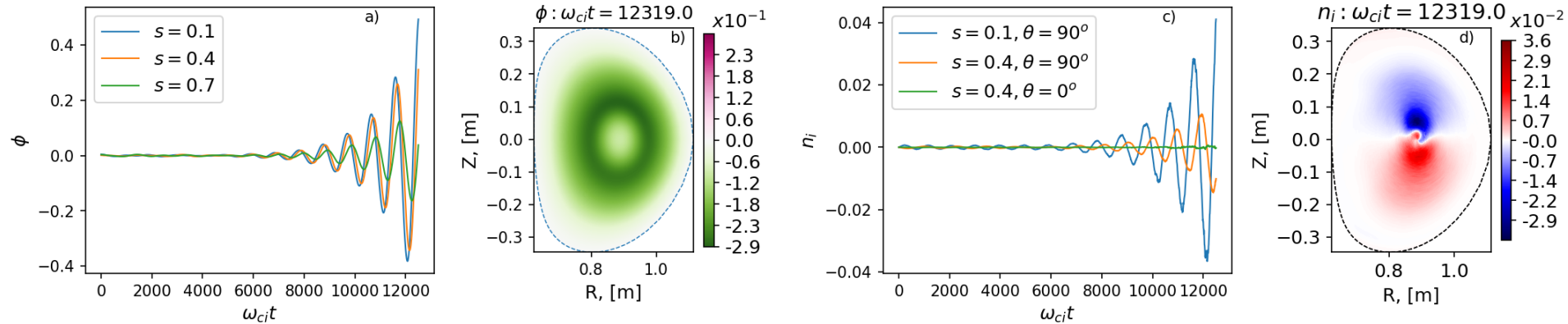


Fig.6 a) evolution of the plasma potential fluctuations at 3 radial positions, b) space distribution of plasma potential fluctuations at $\omega_{ci}t = 12319$, c) evolution of the ion density fluctuations at 2 radial and 2 poloidal positions marked in the legend, d) space distribution of ion density fluctuations at $\omega_{ci}t = 12319$.

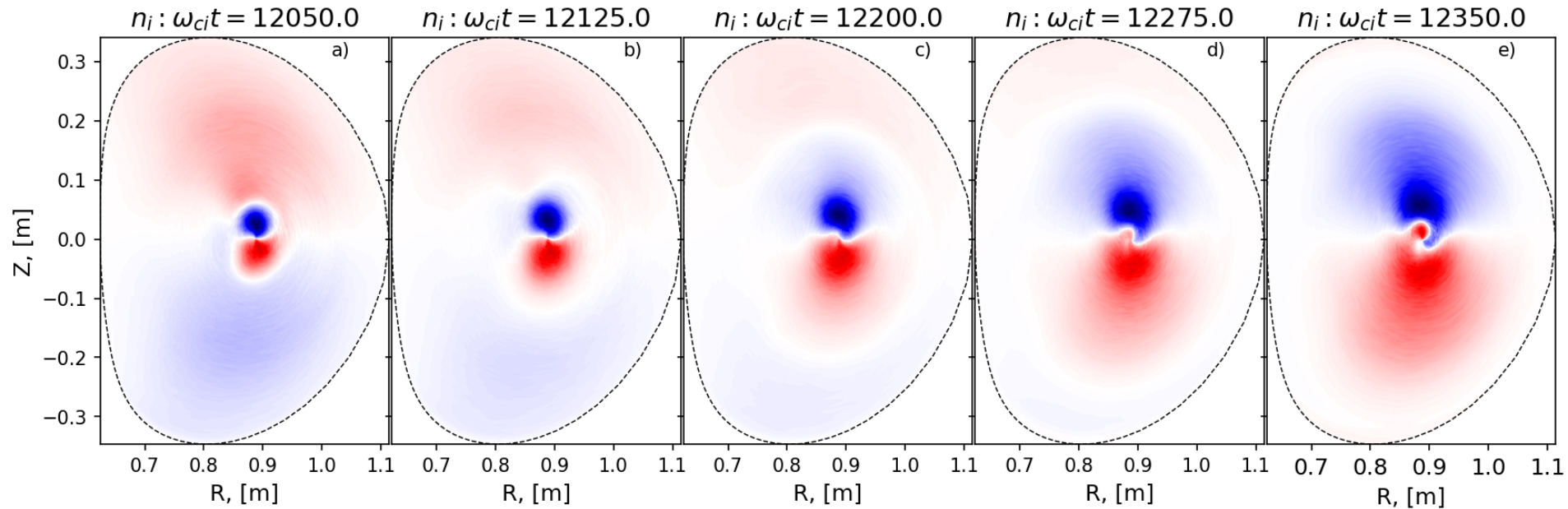
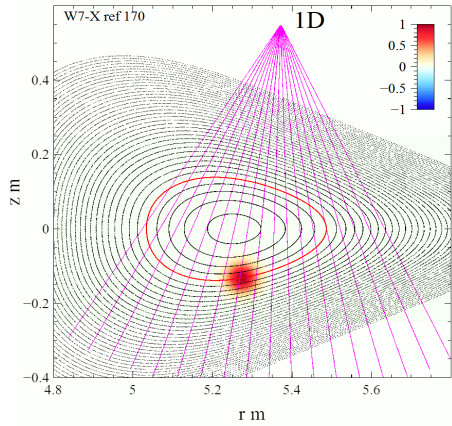
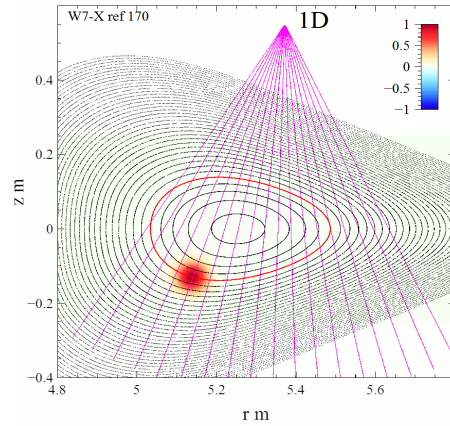
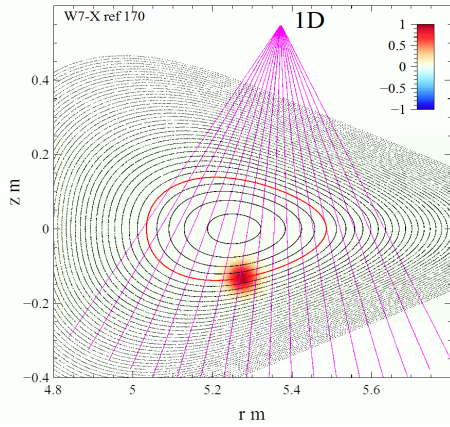
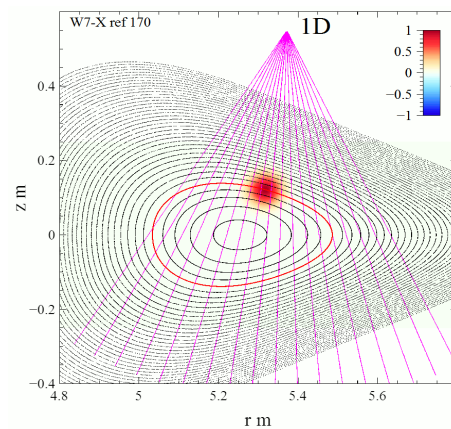
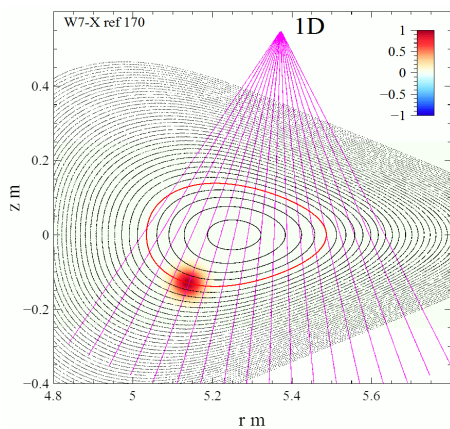
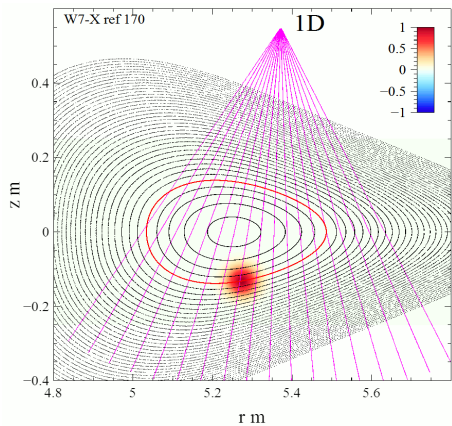
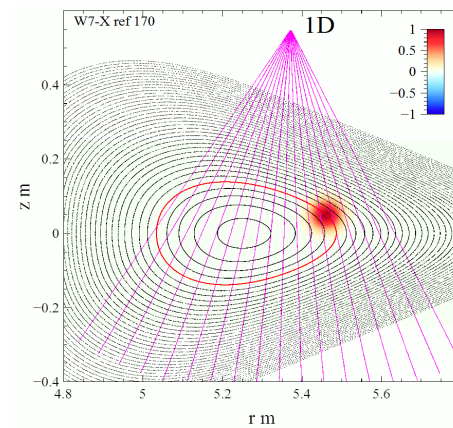
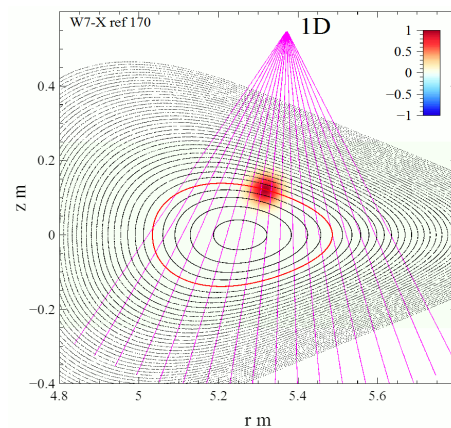
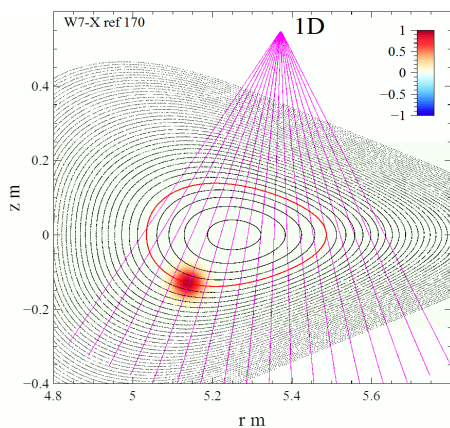
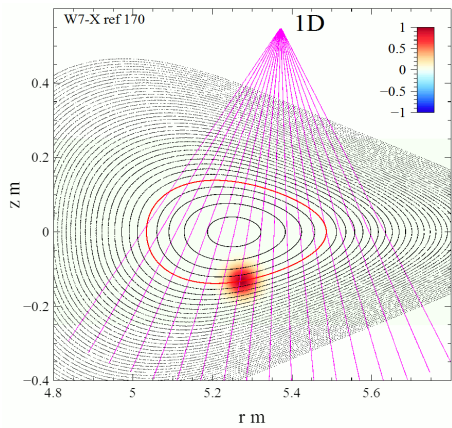


Fig.7 Space distribution of plasma density fluctuations at different moments $\omega_{ci}t$.

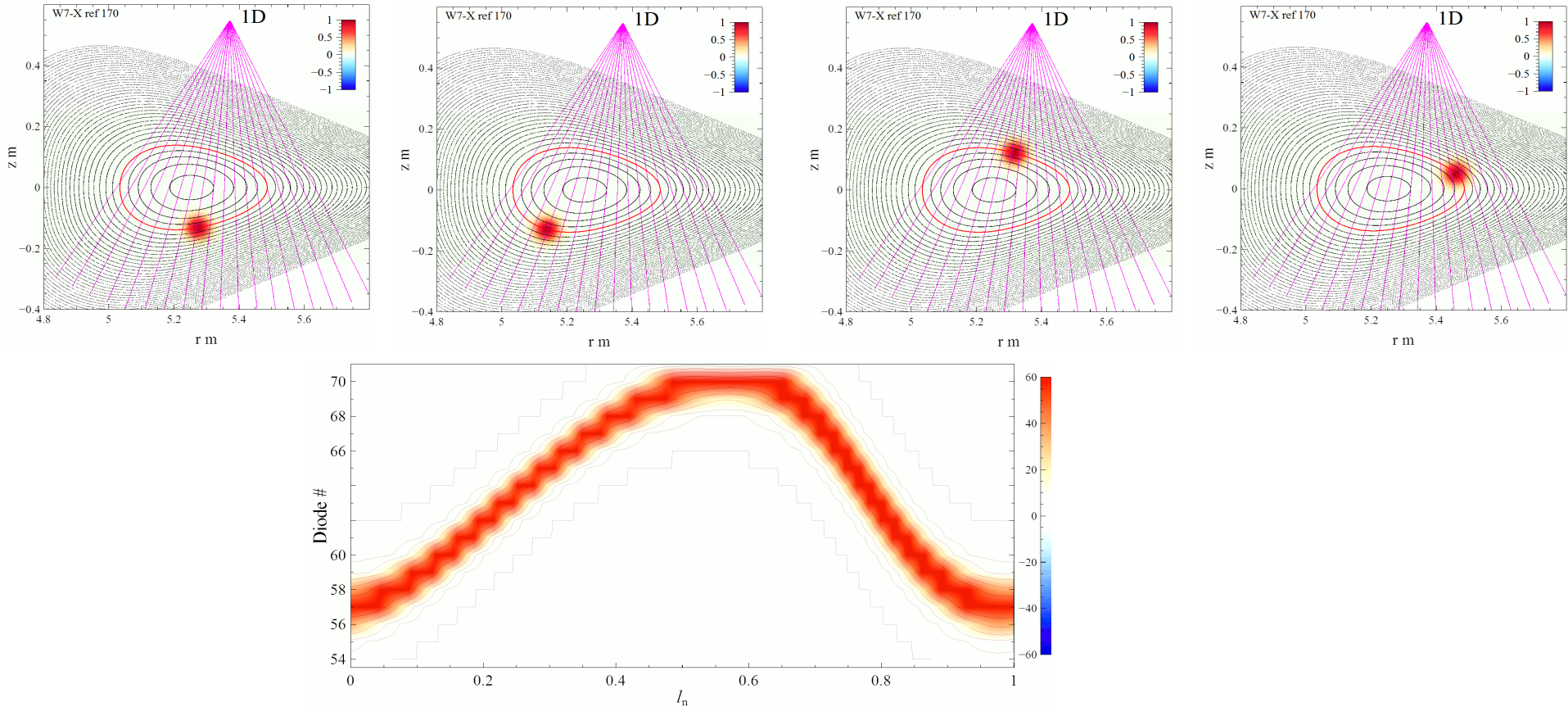








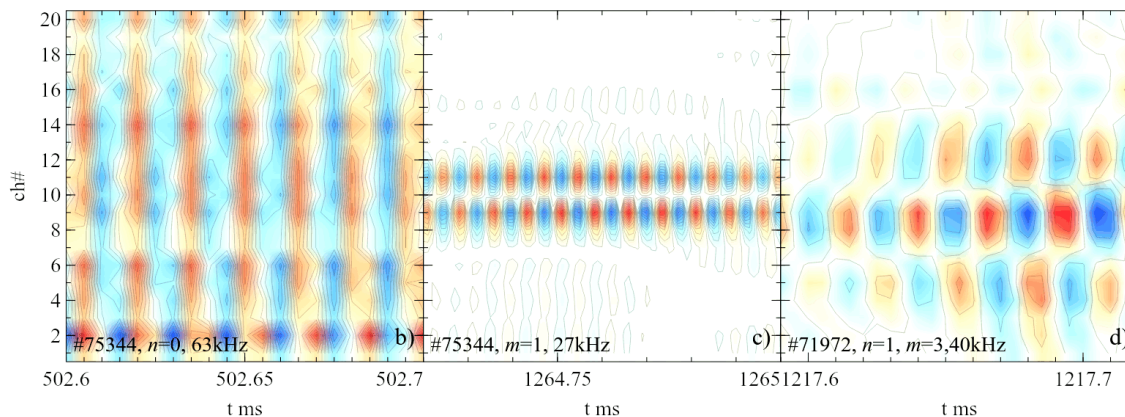
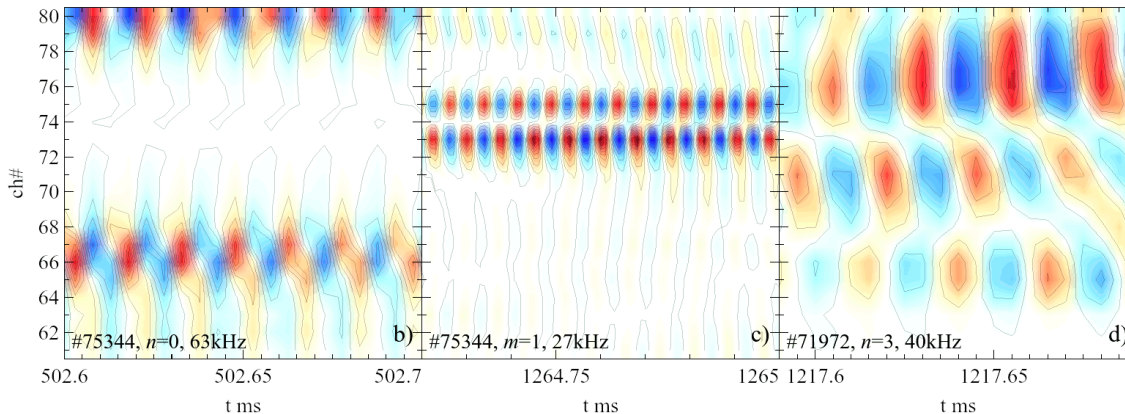
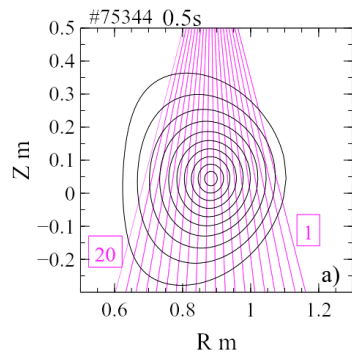
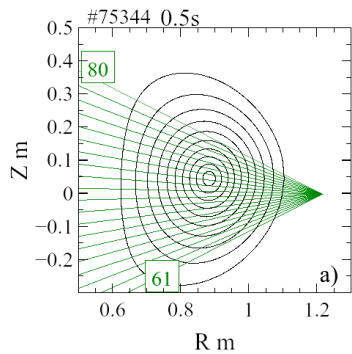
Introduction: SXR spatiotemporal plot and forward modeling

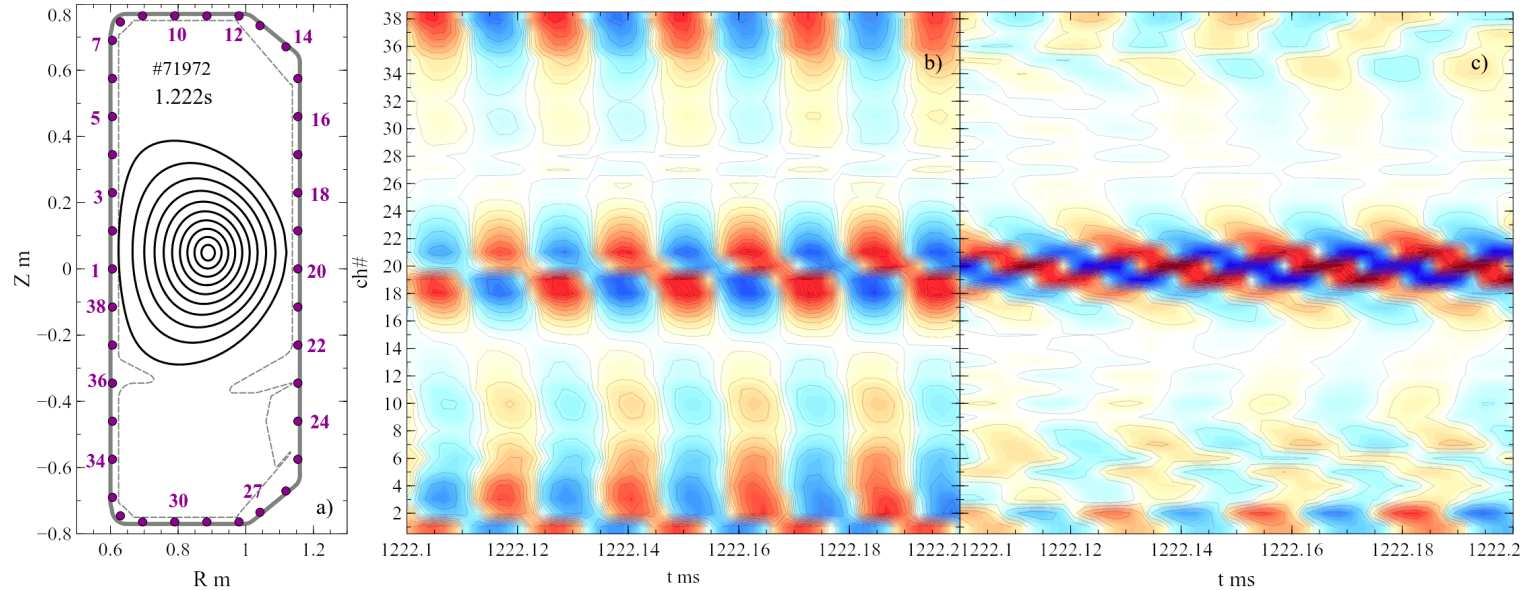


¹Dreval M B et al 2021 Plasma Phys. Control. Fusion **63** 065006

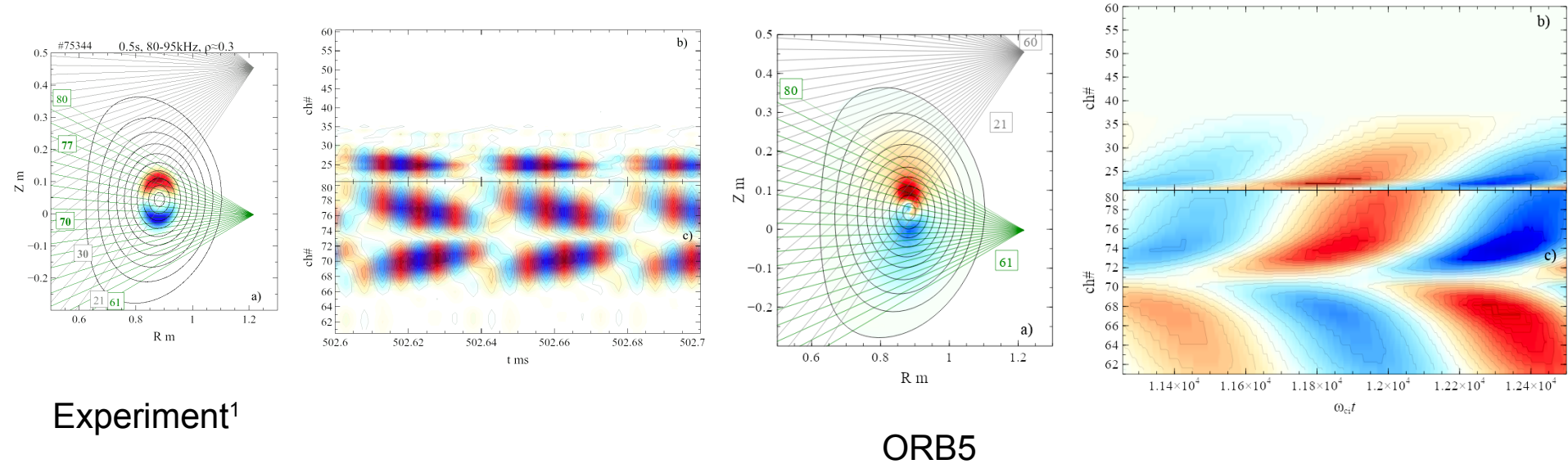
²M B Dreval et al 2023 Plasma Phys. Control. Fusion **65** 035001

EGAM versus rotating mode: SXR





EGAM space structure by ORB5: “SXR” Diagnostics

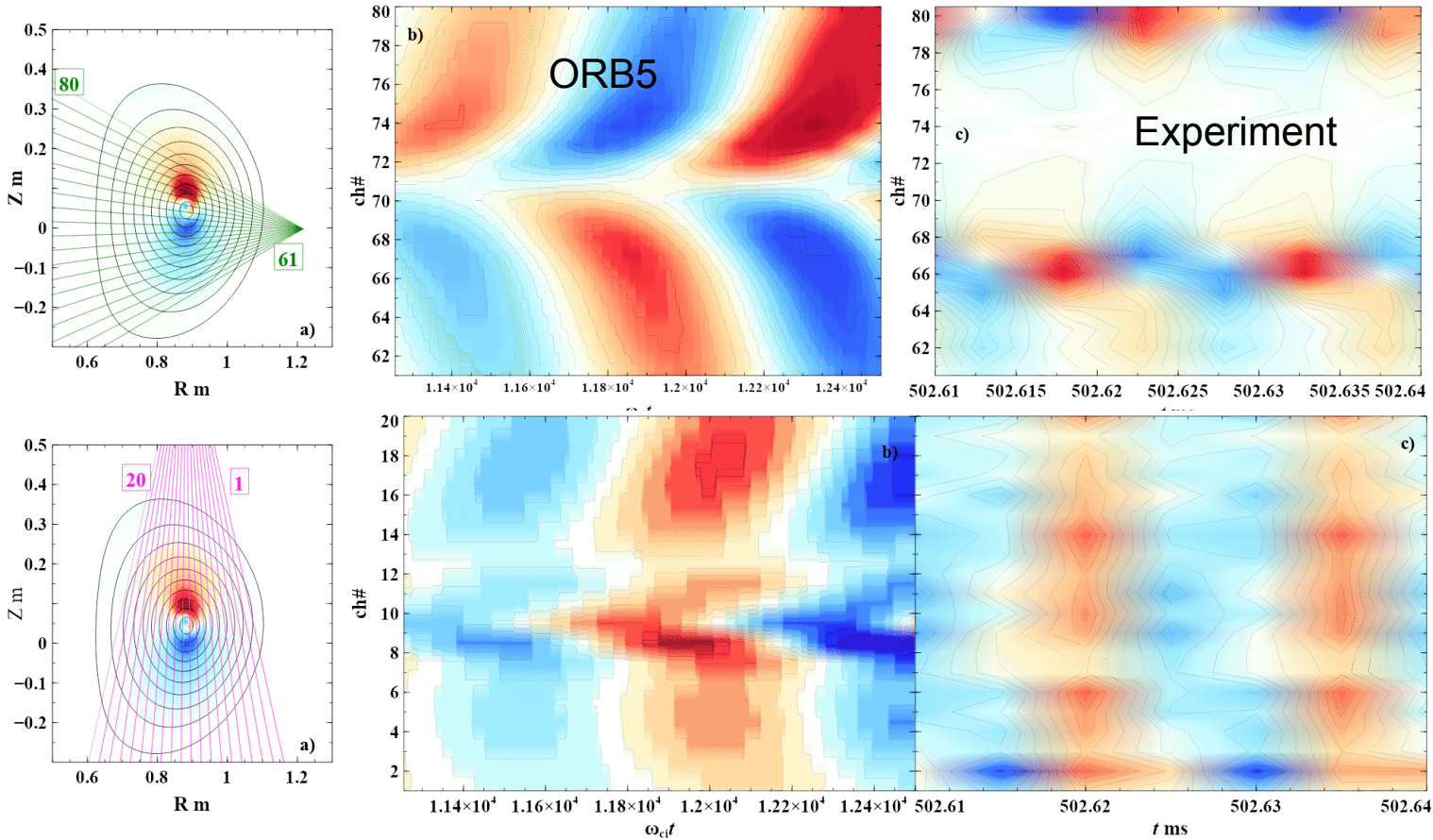


Experiment¹

ORB5

Fig.8 (a) Lines-of-sight of the AXUV side camera in green, top-side camera in gray across the magnetic flux surfaces in TCV discharge #75344 at 0.5 s and EGAM ion density perturbations distribution calculated by ORB5; (b),(c) Spatiotemporal evolution of emission data obtained by integration of ORB5 EGAM ion density perturbation along lines of sights of top-side and side AXUV cameras.

EGAM space structure by ORB5: "SXR" Diagnostics





Two simultaneous EGAMs

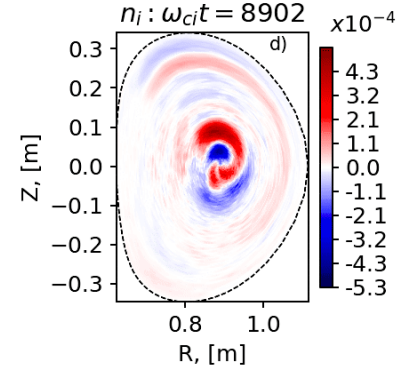
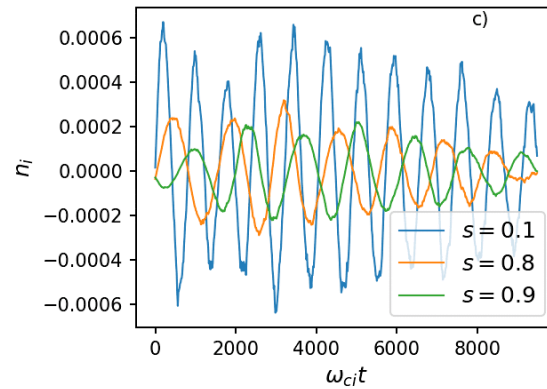
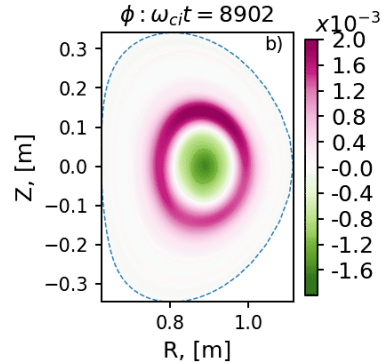
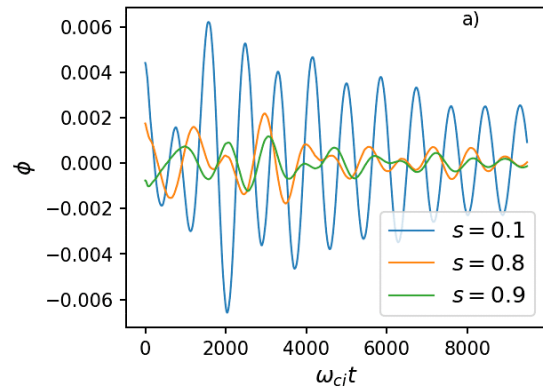
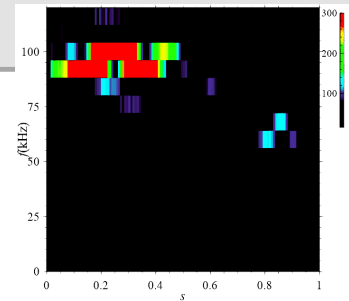


Fig.10 a) evolution of the plasma potential fluctuations at 3 radial positions, b) space distribution of plasma potential fluctuations at $\omega_{ci}t = 8902$, c) evolution of the ion density fluctuations at 3 radial positions marked in the legend, d) space distribution of ion density fluctuations at $\omega_{ci}t = 8902$.



In the present work, we model the spatial structure of the EGAM modes in the TCV equilibrium using a **realistic fast ion distribution function**, implemented in the gyrokinetic particle-in-cell code ORB5. For a peaked radial profile of fast ions, the EGAM spatial structure coincides with that of the conventional GAM, characterized by an **$n/m=0/0$ plasma potential** perturbation and an **$m=1$ standing perturbation**, where the amplitude of the **density** oscillations is proportional to the sine of the poloidal angle. In contrast, for a hollow radial profile of fast ions, our simulations reproduce a **complex EGAM spatial structure**—similar to that observed experimentally in TCV—with two coexisting frequencies.

³M.B. Dreval et al., 2025 Nucl. Fusion **65** 016037

⁴M.B. Dreval et al., EUROfusion pinboard 2025 #589